ACS APPLIED MATERIALS & INTERFACES

Research Article

www.acsami.org

Toward Infection-Resistant Surfaces: Achieving High Antimicrobial Peptide Potency by Modulating the Functionality of Polymer Brush and Peptide

Kai Yu,[†] Joey C. Y. Lo,[‡] Yan Mei,[†] Evan F. Haney,[§] Erika Siren,[⊥] Manu Thomas Kalathottukaren,[†] Robert E.W. Hancock,[§] Dirk Lange,[‡] and Jayachandran N. Kizhakkedathu*[,†,⊥]

[†]Centre for Blood Research and Department of Pathology & Laboratory Medicine and [⊥]Department of Chemistry, University of British Columbia, Vancouver, British Columbia V6T 1Z3, Canada

[‡]Department of Urologic Sciences, University of British Columbia, Vancouver, British Columbia V5Z 1M9, Canada

[§]Department of Microbiology and Immunology and Centre for Microbial Diseases and Immunity Research, University of British Columbia, Vancouver, British Columbia V6T 1Z4, Canada

Supporting Information

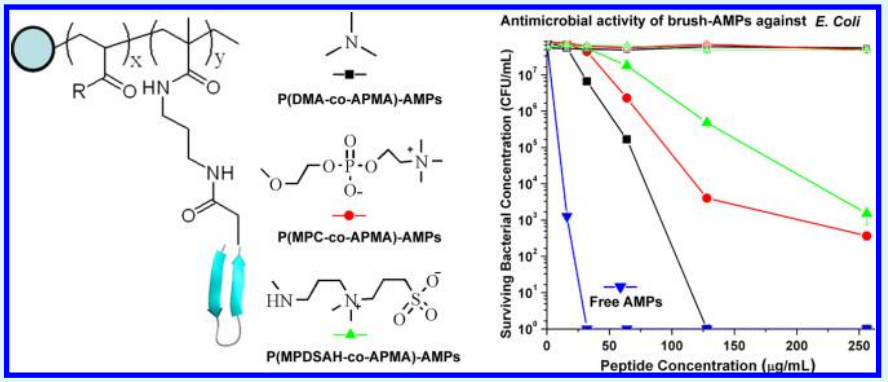

ABSTRACT: Bacterial infection associated with indwelling medical devices and implants is a major clinical issue, and the prevention or treatment of such infections is challenging. Antimicrobial coatings offer a significant step toward addressing this important clinical problem. Antimicrobial coatings based on tethered antimicrobial peptides (AMPs) on hydrophilic polymer brushes have been shown to be one of the most promising strategies to avoid bacterial colonization and have demonstrated broad spectrum activity. Optimal combinations of the functionality of the polymer-brush-tethered AMPs are essential to maintaining long-term AMP activity on the surface. However, there is limited knowledge currently available on this topic. Here we report the development of potent antimicrobial coatings on implant surfaces by elucidating the roles of polymer brush chemistry and peptide structure on the overall antimicrobial activity of the coatings. We screened several combinations of polymer brush coatings and AMPs constructed on nanoparticles, titanium surfaces, and quartz slides on their antimicrobial activity and bacterial adhesion against Gram-positive and Gram-negative bacteria. Highly efficient killing of planktonic bacteria by the antimicrobial coatings on nanoparticle surfaces, as well as potent killing of adhered bacteria in the case of coatings on titanium surfaces, was observed. Remarkably, the antimicrobial activity of AMP-conjugated brush coatings demonstrated a clear dependence on the polymer brush chemistry and peptide structure, and optimization of these parameters is critical to achieving infection-resistant surfaces. By analyzing the interaction of polymer-brush-tethered AMPs with model lipid membranes using circular dichroism spectroscopy, we determined that the polymer brush chemistry has an influence on the extent of secondary structure change of tethered peptides before and after interaction with biomembranes. The peptide structure also has an influence on the density of conjugated peptides on polymer brush coatings and the resultant wettability of the coatings, and both of these factors contributed to the antimicrobial activity and bacterial adhesion of the coatings. Overall, this work highlights the importance of optimizing the functionality of the polymer brush to achieve infection-resistant surfaces and presents important insight into the design criteria for the selection of polymers and AMPs toward the development of potent antimicrobial coating on implants.

KEYWORDS: *infection-resistant surfaces, polymer brush coating, antimicrobial peptides, bacterial adhesion, antimicrobial activity, polymer brush chemistry*

1. INTRODUCTION

Biofouling of implanted medical devices by bacterial biofilms that seed subsequent infections greatly compromises the long-term

Received: October 21, 2015
Accepted: December 7, 2015
Published: December 7, 2015

DOI: 10.1021/acsami.5b10074
ACS Appl. Mater. Interfaces 2015, 7, 28591−28605

performance and stability of the implant and is associated with significant morbidity and mortality.[1−4] The use of novel biocompatible coatings with broad-spectrum antimicrobial activity has previously been shown to be an effective strategy for preventing device-associated infections.[5−7] While research into this area is promising, coatings with optimal biocompatibility and antimicrobial activity must be elucidated. Covalent coatings based on hydrophilic polymer brushes offer a promising approach to preventing initial bacterial adhesion to the device surface because of its ability to provide a steric barrier against bacterial adhesion and colonization.[8−14] Immobilization of antimicrobial agents onto polymer brushes has previously been shown to be highly effective in preventing bacterial biofilm formation on device surfaces because both the steric hindrance offered by the polymer brushes and the direct killing by the antimicrobial agent prevent the interaction of live bacteria with the device surface.[15−26] While the effectiveness of different antimicrobial agents has previously been investigated, no information exists on whether the polymer brush chemistry can influence the activity of immobilized antimicrobial agents on the surface. The present study was aimed at investigating the effects of different polymer brush chemistries on the activity of an immobilized antimicrobial agent. The findings from these studies are important for future antimicrobial medical biomaterial design and will facilitate the development of coatings with optimal antibiofouling activity.

Antimicrobial peptides (AMPs) represent an excellent choice for antimicrobial agents with broad-spectrum activity against bacteria, fungi, and viruses, making them a good alternative to current antimicrobials.[27−33] AMPs are amphipathic peptides that carry a net positive charge at physiological pH and structurally contain a significant proportion (∼50% or more) of hydrophobic amino acids. The antimicrobial activity of AMPs has been attributed, in part, to the ability of cationic peptides to disrupt the integrity of the negatively charged bacterial membrane.[34−36]

Previous studies have shown that grafted coatings consisting of AMPs tethered to polymer brushes with antifouling characteristics result in the uniform distribution of covalently attached AMPs, which significantly decreases the accumulation of bacteria on implant surfaces.[18−24] To date, various types of polymer brushes with neutral and zwitterionic characteristics have been shown to prevent nonspecific protein and bacterial adhesion on surfaces.[9−15] The nonfouling characteristics of such surface coatings depend on their hydrophilicity/hydrophobicity and steric repulsion offered by the surface-grafted chains.[8−13] There are also a variety of natural or synthetic AMPs reported that show excellent antimicrobial activity in the soluble form.[27−33] However, AMP conjugation to polymer brushes or polymer coatings with good nonfouling properties will not always result in potent antimicrobial surfaces.[21,22,37] The structure−activity relationships that dictate peptide antimicrobial activity in its soluble form are not always applicable to tethered peptides[38] because in complex media a multitude of surface interactions contribute to bacterial adhesion and protein interactions that dictate the overall antimicrobial activity of the surface. For instance, the net positive charge on the surface contributes to an initial bacterial adhesion, and a higher positive charge density results in stronger adhesion. There is, however, not much known about how a tethered peptide structure or hydrophilicity of the surface affects the overall antimicrobial activity. Thus, the effect of the AMP structure on the activity for polymer-tethered peptides needs to be further investigated and established.

Previous studies focused on using single-polymer-brush systems and different AMPs to construct the antimicrobial surface.[5−8,24−26] There is limited information available on how the brush chemistry and structure (nonfouling component) contribute to the interaction of conjugated AMPs and how these parameters influence their overall antimicrobial activity. Improving our understanding on how these factors interplay and contribute to the overall antimicrobial activity is key in our ability to design the most efficacious antimicrobial surface for a given application. Thus, here we investigated the influence of the polymer brush chemistry and peptide structure on the antimicrobial activity of peptides conjugated to various polymer brush coated surfaces. We found that the degree of change in the peptide secondary structure upon its interaction with the bacterial membrane was significantly impaired in certain cases, influencing the overall antimicrobial activity of surfaces containing polymer-brush-tethered AMPs. The brush chemistry, peptide hydrophilicity, and density all contributed to the antimicrobial activity of AMP tethered surfaces. Taken together, this work represents an important step toward the design of highly effective antimicrobial coatings based on polymer brushes and AMPs toward infection-resistant implants.

2. EXPERIMENTAL SECTION

2.1. Materials. [3-[(Methacryloyl)amido]propyl]dimethyl(3-sulfopropyl)ammonium hydroxide inner salt (96%), 2-[(methacryloyl)-oxy]ethylphosphorylcholine (97%), 1,1,4,7,10,10-hexamethyltriethylenetetramine (97%), tris[2-(dimethylamino)ethyl]amine (Me_6TREN; 97%), methyl 2-chloropropionate (97%), a sodium methoxide (NaOMe) solution (25 wt % in methanol), CuCl (99%), and $CuCl_2$ (99%) were purchased from Sigma-Aldrich (Oakville, Ontario, Canada). *N*-(3-Aminopropyl)methacrylamide hydrochloride (APMA; 98%) was purchased from Polysciences, USA, and used as supplied. *N*,*N*-Dimethylacrylamide (DMA; 99%, Aldrich) was distilled under reduced pressure before use. Water was purified using a Milli-Q Plus water purification system (Milipore Corp., Bedford, MA) and used in all experiments. All other reagents were purchased from Sigma-Aldrich and used without further purification. A single-side-polished silicon wafer (University Wafer, Boston, MA) deposited with titanium (∼250 nm) was prepared by e-beam evaporation of titanium (physical vapor deposition). The process was progressed in a home-assembled Evaporator 2000 system equipped with a quartz crystal microbalance to monitor the film thickness and a cryo pump to reach high-vacuum (10^{-7}−10^{-6} Torr) conditions. After deposition, the substrates were washed with Milli-Q water, dried via a N_2 gun, and stored for further usage. Cysteine-containing peptides were synthesized by CanPeptide Corp. (>95% purity by high-performance liquid chromatography; Montreal, Quebec, Canada) and used as supplied. Quartz slides (76.2 × 25.4 × 1.0 mm) were purchased from Alfa Aesar (Haverhill, MA) and cut into 38.1 × 8.0 × 1.0 mm before use. [11-[(2-Bromo-2-methylpropionyl)oxy]undecyl]trichlorosilane and deposition of the surface initiator onto the silicon wafer or titanium surface was done using a procedure similar to that reported in the literature.[39] Atom-transfer radical polymerization (ATRP) initiator-modified polystyrene (PS) particles (597 ± 6.2 nm) were synthesized by a shell growth mechanism utilizing surfactant-free emulsion polymerization of styrene and 2-(methyl-2′-chloropropionato)ethyl acrylate.[40] Iodoacetic acid *N*-hydroxysuccinimide ester was synthesized using a procedure similar to that reported in the literature.[41]

2.2. Instrumentation. *2.2.1. Ellipsometry.* The variable-angle spectroscopic ellipsometry (VASE) spectra were collected on an M-2000 V spectroscopic ellipsometer (J. A. Woollam Co. Inc., Lincoln, NE) at 50°, 60°, and 70° at wavelengths from 480 to 700 nm with an M-2000 50 W quartz tungsten halogen light source. The VASE spectra were then fitted with a multilayer model utilizing *WVASE32* analysis software, based on the optical properties of a generalized Cauchy layer to obtain the dry thickness of the polymer brush layers. The graft density σ was

DOI: 10.1021/acsami.5b10074
ACS Appl. Mater. Interfaces 2015, 7, 28591−28605

calculated according to $\sigma = N_A h\rho/M_n$, where M_n is the number-average molecular weight, N_A is Avogadro's number, and ρ is the density for the dry polymer. The polymer layer thickness in an aqueous medium was determined using a four-layer model (water, polymer, silicon oxide, and silicon) with a fixed incidence angle at 70°. Measurements were made in chambers that had no significant window effects. These values were obtained by using the Woollam *CompleteEASE* program to fit data obtained for a calibration silicon wafer having a relatively thick oxide layer. An initial measurement was made with the calibration wafer in air to determine the oxide layer thickness (23.45 nm), which was assumed to remain constant. The only variables remaining for the fitting of the data obtained in water were therefore the Cauchy coefficients for the ambient medium. The values thus obtained were used to estimate the thicknesses of the polymer brush layers in aqueous conditions.

2.2.2. Fourier Transform Infrared (FTIR). FTIR absorption spectra of an AMP tethered brush surface were collected on a Nexus 670 FTIR ESP spectrometer (Nicolet Instrument Corp., Waltham, MA) with a MCT/A liquid-nitrogen-cooled detector, a KBr beam splitter, and a MkII Auen Gate single-reflection attenuated-total-reflectance accessory (Specac Inc., Woodstock, GA). Spectra were recorded at 4 cm^{-1} resolution, and 128 scans were collected. The modified nanoparticles (NPs) were mixed with KBr powder with a mass ratio of 1:100, then manually ground in a mortar, and subsequently pressed to prepare semitransparent KBr pellets.

2.2.3. Water Contact-Angle Measurements. A water droplet (6 uL) was placed on the surface, and an image of the droplet was taken with a digital camera (Retiga 1300, Q-imaging Co.). The contact angle was analyzed using *Northern Eclipse* software. Over three different sites were tested for each sample.

2.3. Synthesis of Poly(*N*,*N*-dimethylacrylamide) (PDMA)-*co*-APMA Brushes on PS NPs. Initiator-modified PS particles (60 mg), nonionic surfactant Brij 35 (3.3 mg), and Milli-Q water (2.5 mL) were added successively into a glass tube, which was then degassed by three freeze−pump−thaw cycles. The PS particles were dispersed in water homogeneously by subjecting the tube to ultrasonication for 15 min before transferring it to the glovebox. In a separate glass tube, CuCl (6 mg), $CuCl_2$ (1.3 mg), and Me_6TREN (60 μL) were added successively, followed by the addition of Milli-Q water (6 mL). The glass tube was degassed by three freeze−pump−thaw cycles and transferred to the glovebox. DMA (266 μL) and APMA (94 mg) were added to the prepared solution (6 mL). After the monomer was dissolved, 2.5 mL of the solution was mixed with 2.5 mL of the previously prepared PS particle suspension. Soluble methyl 2-chloropropionate (10 μL from a stock solution of 40 μL in 5 mL of methanol) was added to the reaction solution. The suspension was stirred continuously, and polymerization was allowed to proceed at room temperature (22 °C) for 2 h. The polymer-grafted PS particles were rinsed by three repeated cycles of centrifugation (10 min for 16000*g*) and resuspension in a $NaHSO_3$ solution (50 mM) and water to remove adsorbed copper complexes. Finally, the latex suspension was rinsed with a 0.1 M ethylenediaminetetraacetic acid solution three times, followed by another three times with water to remove any copper complex remaining within the grafted surface. poly[[2-[(methacryloyl)oxy]ethyl]-phosphorylcholine] (PMPC)-*co*-APMA brushes were grafted onto PS NPs using similar procedures by adding 500 mg of MPC and 94 mg of APMA. Soluble methyl 2-chloropropionate (20 μL from a stock solution of 40 μL in 5 mL of methanol) was added to the reaction solution, and the reaction was left for 24 h. poly[3-[(methacryloyl)amido]propyl-*N*,*N*-dimethyl(3-sulfopropyl)ammonium hydroxide] (PMPDSAH)-*co*-APMA brushes were grafted onto PS NPs by adding MPDSAH (500 mg) and APMA (61 mg) into a 0.5 M NaCl solution. Soluble methyl 2-chloropropionate (20 μL from a stock solution of 40 μL in 5 mL of methanol) was added to the solution, and the reaction was left for 2 h. All grafted structures were characterized in terms of the thickness, grafting density, molecular weight, and polydispersity.

2.4. Synthesis of PDMA-*co*-APMA Brushes on Quartz Slides and Titanium Surface. The quartz slides were first deposited with a surface initiator ([11-[(2-bromo-2-methylpropionyl)oxy]undecyl]-trichlorosilane) using a procedure similar to that reported in the literature.[36] The initiator-modified quartz slide was subjected to hydrolysis (using 25% NaOMe for 30 s) to decrease the initiator density on the surface. Copper(II) chloride ($CuCl_2$; 1.5 mg), copper(I) chloride (CuCl; 10 mg), and Me_6TEN (60 μL) were added successively into a glass tube, followed by the addition of 20 mL of Milli-Q water. The solution was degassed with three freeze−pump−thaw cycles and then transferred into the glovebox. The catalyst solution (10 mL) was thoroughly mixed before the addition of DMA (180 μL) and APMA (62.5 mg). The modified quartz slides were immersed in the polymerization mixture. Soluble methyl 2-chloropropionate (36 μL from a stock solution of 40 μL in 5 mL of methanol) was added immediately to the reaction mixture, and the polymerization was allowed to proceed at room temperature (22 °C) for 2 h. The substrate was then rinsed thoroughly with Milli-Q water and sonicated in water for 10 min. The soluble polymer formed along with the surface-grafted polymer was collected by dialysis (molecular weight cutoff: 1000) against water for 1 week.

PMPC-*co*-APMA brushes were grafted onto quartz slides using similar procedures by adding MPC (663 mg) and APMA (125 mg) into the catalyst solution (10 mL). Soluble methyl 2-chloropropionate (8 μL from a stock solution of 40 μL in 5 mL of methanol) was added immediately to the reaction mixture, and the reaction was left at room temperature for 24 h. The initiator-modified quartz slide (without further hydrolysis) was used.

PMPDSAH-*co*-APMA brushes were grafted onto a quartz slides using similar procedures by adding MPDSAH (1060 mg) and APMA (123 mg) into the catalyst solution (10 mL). Soluble methyl 2-chloropropionate (8 μL from a stock solution of 40 μL in 5 mL of methanol) was added immediately to the reaction mixture and the reaction proceeded for 2 h. The initiator-modified quartz slide (without further hydrolysis) was used.

PDMA-*co*-APMA, PMPDSAH-*co*-APMA, and PMPC-*co*-APMA brushes were grafted onto titanium surfaces using a similar procedure. The experimental details were described in the Supporting Information. The surfaces are copper-free, as revealed by X-ray photoelectron spectroscopy (Figure S8 in the Supporting Information).

2.5. Peptide Conjugation onto Polymer-Brush-Modified PS NPs. Polymer-brush-modified PS NPs (20 mg) were well-dispersed in 20 mL of PBS buffer (137 mM sodium chloride, 2.7 mM potassium chloride, 10 mM disodium hydrogen phosphate, and 1.8 mM potassium dihydrogen phosphate). Iodoacetic acid *N*-hydroxysuccinimide ester (16 mg) was added, and the pH was adjusted to between 7 and 7.5. After 2 h, the reaction was stopped by centrifugation (10 min at 16000*g*). The NPs were rinsed by three repeated cycles of centrifugation and dried under vacuum. Linker (iodoacetic acid *N*-hydroxysuccinimide ester)-modified PS NPs (20 mg) were then dispersed in 3 mL of PBS buffer. Peptide without amidation at the C-terminus (either E6 with sequence RRWRIVVIRVRRC or Tet20 with sequence KRWRIRVRVIRKC) was dissolved in PBS buffer at a concentration of 1 mg/mL and added into the NP suspension. The reaction was kept overnight and then stopped by centrifugation. The particles were then rinsed with three repeated cycles of centrifugation (10 min at 16000*g*) and washing and dried under vacuum.

2.6. Peptide Conjugation onto Polymer-Brush-Modified Quartz Slides and Titanium Surface. Polymer-brush-modified quartz slides and titanium surface were immersed in 10 mL of PBS buffer. Iodoacetic acid *N*-hydroxysuccinimide ester (8 mg) was added, and the pH was adjusted to between 7 and 7.5. The reaction proceeded overnight. Substrates were then rinsed in PBS buffer, sonicated in water for 5 min, and dried under an argon flow. The linker (iodoacetic acid *N*-hydroxysuccinimide ester)-modified substrates were immersed in the peptide solution in 100 mM phosphate buffer (61 mM disodium hydrogen phosphate and 39 mM potassium dihydrogen phosphate) at 1 mg/mL overnight followed by incubation with an excess of 1-thioglycerol (30 μL/mL) for another 1 day. The peptide-immobilized quartz slide and titanium surface were thoroughly rinsed with 100 mM phosphate buffer and Milli-Q water consecutively and dried under an argon flow.

2.7. Antimicrobial Testing of AMPs Tethered to NPs. The antimicrobial activity of NPs was assessed using a static microtiter plate assay. Briefly, bacteria [*Pseudomonas aeruginosa* lux strain (PAO1

DOI: 10.1021/acsami.5b10074
ACS Appl. Mater. Interfaces 2015, 7, 28591−28605

Tn7::Plac-lux), *Staphylococcus aureus* lux strain (Xen36 Lux), and *Escherichia coli* lux strain (DH5-α, plasmid pUC 19)] were grown in Lysogeny broth (LB; 10 g of tryptone, 5 g of yeast extract, and 10 g of NaCl/L) from freezer stocks at 37 °C O/N, subcultured, and used at approximately 5×10^5 CFU/mL (CFU = colony-forming unit), as determined by OD_{600} readings using the approximate equation of $0.1OD_{600} = 10^8$ CFU/mL. 96-well plates (Corning 96 well white flat bottom PS untreated microplate, product 3912) were sterilized for 30 min under UV light and used for the NP testing. Peptide-conjugated brush-coated, unmodified brush-coated, and uncoated NPs were diluted to 512 μg/mL (AMP concentration) followed by serial doubling dilutions in a minimal basal medium 2 glucose medium [BM2; 62 mM potassium phosphate buffer, pH 7, 7 mM $(NH_4)_2SO_4$, 2 mM $MgSO_4$, 10 μM $FeSO_4$, and 0.4% (w/v) glucose] across the sterile 96-well plate to obtain concentrations of 512, 256, 128, 64, 32, 16, 8, 4, 2, 1, and 0.5 μg/mL AMP equivalent in columns 1−11. A BM2 medium containing 0 μg/mL of NPs was added to the last column to serve as the control. All concentrations were performed in triplicate per bacterium, and all wells should contain 100 μL of solution at this point. The initial bacteria concentration was determined by CFU analysis and was approximately 1×10^6 CFU/mL. Bacteria (100 μL) resuspended in a BM2 medium was introduced to each well, making a total volume of 200 μL/well and hence further diluting all peptide and bacterial concentrations by half. All of the wells were mixed gently and incubated at 37 °C.

2.7.1. Determining the Bacterial Concentration via Luminescence. At 1, 2, 3, and 4 h postincubation, loaded 96-well plates were transferred to a luminescence reader (Tecan Infinite 200 Pro), and the luminescence levels for each well were determined. All plates were transferred back to the incubator after each reading.

2.7.2. Determining the Bacterial Concentration via CFU Counts. At 4 h postincubation and after the last luminescence reading was performed, all wells were serially diluted 10 times in sterile PBS buffer up to 10^{-5} dilution and spot-plated onto LB agar plates for CFU measurements. All plates were incubated at 37 °C O/N or until visible colonies formed. All colonies and dilutions were recorded to determine the concentration of live bacteria per well.

2.8. Viability of Bacteria on an AMP-Brush-Grafted Titanium Surface. Live/Dead BacLight bacterial viability kit (L-7012; Molecular Probes, Eugene, OR) was used to determine the bacterial cell viability on an AMP-brush-grafted substrate. AMP-brush-grafted and bare titanium substrates were each placed in a 24-well microtiter plate. The samples were then sterilized with 1 mL of 70% ethanol for 5 min. The ethanol solution was removed after every 5 min, and the process was repeated three times. The samples were washed with sterilized water three times. *S. aureus* lux strain (Xen36 Lux) was grown in LB broth (4 mL, pH 7.2) at 37 °C overnight to a concentration of around 10^8 CFU/mL. The bacteria (20 μL) were then diluted by a BM2 medium (12 mL). A diluted bacteria suspension (1 mL) was then introduced to each well, and the substrates were placed on a shaker at a speed of 100 rpm to provide a homogeneous liquid environment for the interaction and incubated at 37 °C for 4 h. The substrates were then washed with 1 mL of PBS buffer consecutively. A solution of the SYTO 9 (0.4 μL) and propidium iodide (PI; 2 μL) dyes in PBS buffer (2 mL) was prepared. After incubation of the substrate with a dye solution at room temperature in a dark environment for 15 min, the substrates were washed with sterilized water and dried. The samples were then examined using a fluorescence microscope (Zeiss Axioskop 2 plus, Thornwood, NY) equipped with a fluorescence illumination system (AttoArc 2 HBO) and appropriate filter sets. Images were randomly acquired on different spots by using a 20× objective lens. The pictures were taken using fluorescein isothiocyanate and rhodamine filters to visualize the bacterial viability. The images were overlaid to generate the merged image by using imageJ 1.48v at an opacity of 50%. The bacteria count using imageJ 1.48v from the merged images was used to determine the total number of adhered bacteria. The bacteria count from the images taken using a rhodamine filter was used to assess the total number of dead bacteria. The antimicrobial activity was calculated by dividing the number of dead bacteria by the total number of bacteria.

2.9. Circular Dichroism (CD) Spectroscopy Analysis of Surface-Immobilized E6. CD spectra of surface-immobilized E6 were collected using a Jasco J-800 spectropolarimeter and a 0.5-cm-path-length quartz cell for quartz surface samples and a 0.2-cm-path-length quartz cell for solution samples. Solution samples with a constant peptide concentration of 0.1 mM were prepared in 1:10 peptide-to-lipid molar ratios, using lipid mixtures of 1:1 DMPC/DMPG. CD analyses of surface-immobilized peptide samples were performed in a similar fashion. A constant lipid concentration of 1.0 mM was prepared by adding 10 mL of 20 mM phosphate buffer solution into the vial containing a dried DMPC/DMPG mixture (DMPC, 6.7 mg; DMPG, 6.9 mg). The formation of a homogeneous lipid solution was achieved by sonication. Then, the lipid solution was pipetted into the quartz cell. The corresponding background samples were run initially without placing the sample quartz slide in the quartz cell. Briefly, the spectra were obtained over a wavelength range of 190−260 nm, using a continuous scanning mode with a response of time of 1 s with 0.5 or 1 nm steps, a bandwidth of 1.5 nm, and a scan speed of 50 nm/min. The signal-to-noise ratio was increased by acquiring each spectrum over an average of three scans. Finally, each spectrum was corrected by subtracting the background from the sample spectrum. The peptide-immobilized quartz slides were directly placed in the quartz cell for CD analysis and then in the sample compartment. The temperature of the sample compartment was kept at 30 °C by means of a water chamber.

3. RESULTS

In the present work, PDMA, PMPC, and PMPDSAH polymers were chosen as the antifouling component of the brush for AMP conjugation because recent studies demonstrated their ability to prevent bacterial and cell adhesion on surfaces.[10−14,21−23] APMA was copolymerized with the respective monomers for the generation of primary amine-functionalized brushes with a copolymer ratio of 5:1 (nonfouling component: PAPMA). All of the copolymer brushes were prepared using surface-initiated atom-transfer radical polymerization (SI-ATRP).[42] The reaction with iodoacetic acid *N*-hydroxysuccinimide ester introduced an iodoacyl group, which was then reacted with the thiol group of the cysteine residue at the C-terminus of AMPs. Two cysteinylated cathelicidin-derived peptides, E6 and Tet20,[22,43] were conjugated to the brushes to construct different combinations of AMP tethered polymer brush coatings prepared on NPs, titanium surfaces, and quartz slides. These different surfaces were used to investigate their influence on AMP tethered brushes and the antimicrobial activity against planktonic and surface-adhered bacteria. CFU counting, luminescence inhibition assay, and live/dead stain assay were used to examine the variability of planktonic and adhered bacteria on the surface. CFU counting is the standard method to access the viability of bacteria and is a sensitive technique. Luminescence inhibition assay due to the integrated lux reporter gene shows the metabolic activity of live bacteria, which can be easily monitored by detection of the luminescence. It provides a way to rapidly screen the activity of AMPs conjugated onto the surface using luminescent bacteria and also shows a good correlation with CFU measurements.[43] The live/dead stain method assesses the viability of the bacteria by examining the membrane integrity using two suitable nucleic acid dyes. By the careful choice of the staining dyes and staining conditions, it is possible to prevent a discrepancy with the other bacterial cell viability methods and to obtain a reliable assessment of the viability of the surface-adhered bacteria.[44,45] As an initial antimicrobial screen to identify the most efficacious peptide, AMPs were conjugated to NPs using the various polymer brushes, and the reduction in the growth of planktonic bacteria exposed to NPs ± polymer brush ± AMP was assessed. Furthermore, to study the structural change of peptides upon their interaction with model biomembranes and bacterial adhesion, AMP-conjugated polymer brushes were prepared on

DOI: 10.1021/acsami.5b10074
ACS Appl. Mater. Interfaces 2015, 7, 28591−28605

Scheme 1. Synthesis of AMP Tethered Polymer Brushes on PS NPs (597 ± 6.2 nm)[a]

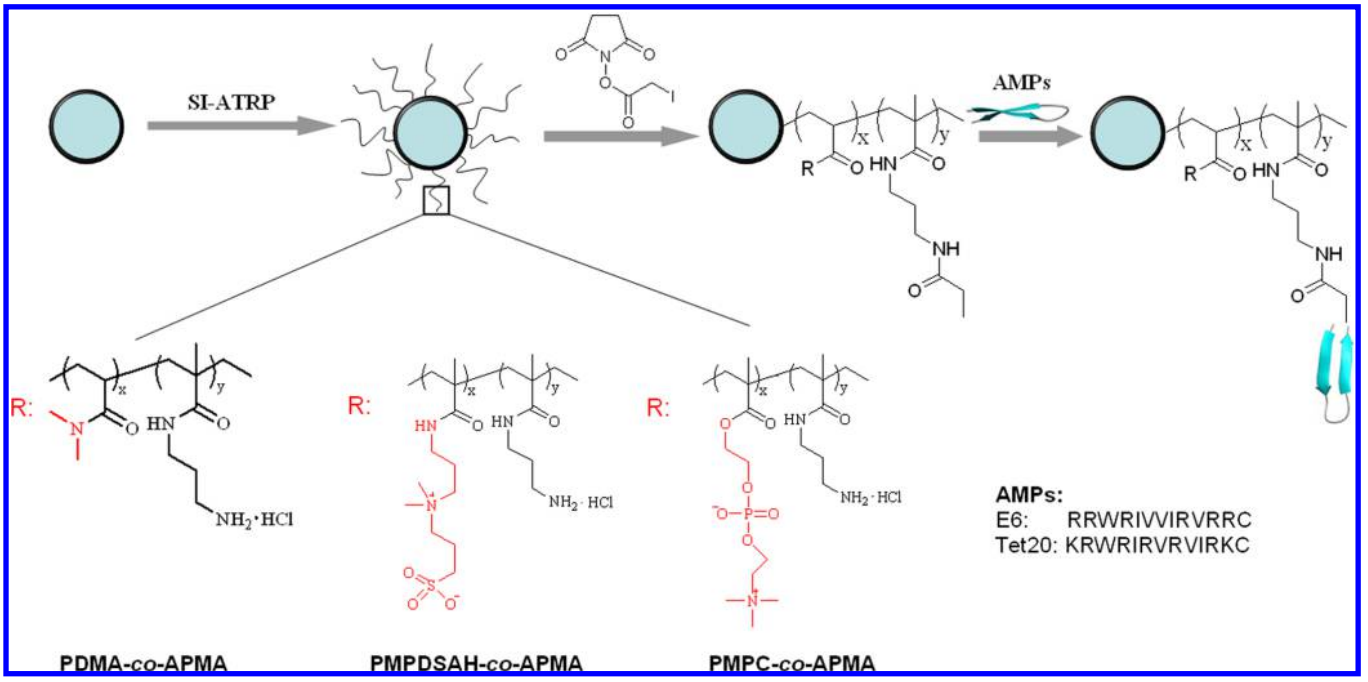

[a]Three different copolymer brushes (PDMA-*co*-APMA., PMPDSAH-*co*-APMA, and PMPC-*co*-APMA) were grafted onto the initiator-modified NPs by SI-ATRP. Peptides E6 (sequence RRWRIVVIRVRRC) and Tet20 (sequence KRWRIRVRVIRKC) were conjugated to the polymer brushes using iodoacetic acid *N*-hydroxysuccinimide ester as a linker.

quartz and titanium surfaces. A combination of surface-specific CD spectroscopy and bacterial live/dead assay was used.

3.1. Synthesis and Characterization of Brush−AMP Conjugates on NPs. To investigate the influence of the polymer brush chemistry and peptide sequence on the antimicrobial activity against planktonic bacteria, polymer brush−AMP conjugates were attached to PS NPs because they possess a high specific surface area (~89660 cm^2/g). This allowed for the unambiguous study of the antimicrobial activity relative to the brush-tethered peptide concentration. Furthermore, the high specific surface area allowed for determination of the AMP density on the surface with high confidence.

An illustration of the synthesis of the polymer brush−AMP system is given in Scheme 1. First, a shell layer of the ATRP initiator was grown on pristine PS NPs,[40] followed by the generation of copolymer brushes of PDMA-*co*-APMA, PMPDSAH-*co*-APMA, and PMPC-*co*-APMA by SI-ATRP.[42] The successful grafting of polymer brushes onto the particle surface was confirmed by FTIR measurements (Figure 1). The appearance of peaks at 1627 and 1550 cm^{-1} was attributed to the C═O stretching and N−H bending vibrations of the amide group of the polymers. The broad peak at 3300 cm^{-1} in the spectrum was due to the stretching of N−H in the amide group. The molar ratio of the polymer components (DMA/APMA, MPDSAH/APMA, and MPC/APMA) in the copolymer brush (Figures S1 and S2 in the Supporting Information) and the grafting density of the brush systems (Table 1) were controlled to be similar to enable direct comparisons between different brushes. Detailed characteristics of the different brushes are given in Table 1. The amine group within the brush system was further modified with iodoacetic acid *N*-hydroxysuccinimide ester, followed by conjugation with the C-terminal cysteine of E6 and Tet20. These peptides were chosen because they not only possessed excellent antimicrobial activity when tethered but also

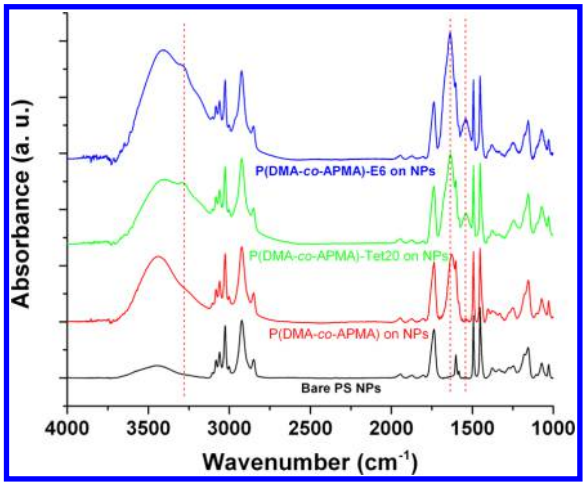

Figure 1. FTIR spectra of AMP tethered PDMA brushes on PS NPs. The appearance of intense peaks at 1627 and 1550 cm^{-1} in the spectrum of PDMA-*co*-APMA on NPs confirmed that the polymer brush was successfully grafted onto the NPs. The increased intensity of 1627 and 1550 cm^{-1} relative to the peak at 1737 cm^{-1} and the presence of the broad peak for amide N−H stretching at 3300 cm^{-1} confirmed the conjugation of AMPs. In addition, the relatively stronger intensity of the peak at 1627 cm^{-1} for PDMA-*co*-APMA−E6 in comparison to PDMA-*co*-APMA−Tet20 suggests a higher peptide density for tethered E6.

were biocompatible.[21,46] The successful conjugation of peptides onto the brushes was evident from the increased intensity of the peaks at 1627 and 1550 cm^{-1} in contrast to the peak at 1737 cm^{-1} in the FTIR spectra of peptide-conjugated brushes (all of the FTIR spectra were normalized to the carbonyl group at 1737 cm^{-1} of the initiator layer on PS NPs to enable direct comparisons). In addition, the increased intensity of the broad

DOI: 10.1021/acsami.5b10074
ACS Appl. Mater. Interfaces 2015, 7, 28591−28605

Table 1. Characteristics of AMP Tethered Polymer Brushes on PS NPs

sample	thickness (nm)[a] before	thickness (nm)[a] after	molecular weight,[b] PDI	grafting density (chains/nm^2)	peptide density (μg/cm^2)
NPs−PDMA-*co*-APMA−E6	14.0 ± 5.7	30.8 ± 8.9	260000, 1.2	0.033	1.88
NPs−PDMA-*co*-APMA−Tet20		26.6 ± 7.3			1.36
NPs−PMPC-*co*-APMA−E6	20.1 ± 10.4	35.4 ± 11.2	380000, 1.3	0.032	1.77
NPs−PMPC-*co*-APMA−Tet20		33.2 ± 12.6			1.38
NPs−PMPDSAH-*co*-APMA−E6	19.3 ± 7.1	35.5 ± 9.1	310000, 1.2	0.037	1.89
NPs−PMPDSAH-*co*-APMA−Tet20		33.3 ± 7.2			1.53

[a]The thickness of the polymer layer before and after peptide conjugation was calculated based on the increase in mass after polymerization and peptide conjugation.[60] [b]Molecular weight of the free polymer generated in solution was used to present the molecular weight of grafted polymer. PDI = polydispersity index.

peak for amide N−H stretching at 3300 cm^{-1} also confirmed peptide conjugation to the brushes.

The AMP density on different brushes was calculated from the increased mass of the particles after peptide conjugation (Table 1). The results showed that all three AMP-conjugated brush systems had similar peptide densities on their surfaces (~1.8 μg/cm^2 for E6 and ~1.5 μg/cm^2 for Tet 20; Table 1). Thus, a direct comparison of the polymer brush chemistry and antimicrobial activity could be made for a given AMP. However, it was noticeable that, for each polymer brush system studied, the density of tethered E6 was higher than that of tethered Tet20, even though these peptides had similar molecular weights.

3.2. Antimicrobial Activity of Surface-Tethered AMPs on NPs: Influence of the Chemistry of the Brushes. The antimicrobial activity of surface-tethered AMPs on the three polymer brush systems (PDMA, PMPC, and PMPDSAH) against Gram-positive (*S. aureus*) and Gram-negative (*E. coli* and *P. aeruginosa*) bacteria was evaluated by two different methods: (i) measurement of the inhibition of luminescence due to the integrated lux reporter gene, which reflected the metabolic activity of bacteria; (ii) measurement of the number of CFUs after 4 h of incubation at 37 °C with 10^6 CFU/mL bacteria. To determine the influence of the brush chemistry, the antimicrobial activity of the tethered AMPs (E6 or Tet 20) against *E. coli* was plotted as a function of the peptide concentration (Figure 2A,B). The brush systems without AMPs showed no bactericidal activity. The minimum inhibitory concentration (MIC) values of surface-tethered AMPs were approximately 4-fold less than those of their soluble analogues (Table 2). Compared to tethered magainin-derived peptides and other cationic peptides,[47−49] which have MIC values of 130−1976 and 80−320 μM, respectively, the tethered E6 on NP surfaces has a lower MIC value of about 72.3 μM, which supports its greater antimicrobial activity. The polymer chains in the brushes are flexible and assume their extended conformation in an aqueous medium because of their hydrophilic nature. Thus, the antimicrobial activity was better conserved using the brush approach rather than other direct immobilization strategies, which often use a spacer between the substrate and C-terminus.[47−49] This is illustrated by the ellipsometric measurements, which showed a 1.7-fold swelling of the AMP-conjugated brush in an aqueous medium, suggesting the flexibility of AMP grafted polymer chains on the surface (Table S1 in the Supporting Information). The flexibility of the polymer chains would provide lateral mobility to tethered AMPs and thus facilitate optimal interactions with bacterial membranes resulting in enhanced bactericidal activity.[5,50]

Another important observation from the data in Figure 2 was that, at similar grafting and peptide densities on the brushes, the polymer brush chemistry influenced the antimicrobial activity of tethered AMPs. As shown, E6 and Tet 20 were more effective on PDMA brushes in a comparison to PMPC or PMPDSAH brushes at identical AMP concentrations. Luminescence measurements further confirmed these findings (Figure S3 in the Supporting Information). At a peptide concentration of 128 μg/mL, PDMA-brush-conjugated E6 showed 100 ± 2.5% killing in comparison to 77.2 ± 8.9% and 65.8 ± 7.6% killing for E6 conjugated to PMPC and PMPDSAH brushes, respectively. Similar observations were made at other peptide concentrations, although the magnitude of bacterial killing varied with the peptide concentration.

Another notable observation was that the antimicrobial potency of tethered peptides was different from that of their soluble counterparts (Figure 2C). Thus, soluble Tet20 was approximately 2-fold more active than E6 (Figure 2A,B); however, polymer-brush-tethered E6 was more active than the tethered Tet20 at all tested peptide concentrations (Figure 2C), confirming the importance of the peptide sequence on the activity of tethered peptides.

Next we investigated whether the observed *E. coli* killing by brush-tethered AMPs could be extrapolated to other bacterial species with different outer envelopes, specifically the Gram-positive *S. aureus* and Gram-negative *P. aeruginosa*. The activity of tethered AMPs remained highly dependent on the type of polymer brush used for conjugation because PDMA-tethered E6 brush showed 2−3 log lower *S. aureus* and *P. aeruginosa* CFU counts compared to the PMPC brush at peptide concentrations higher than 64 μg/mL (Figure 3A,B). AMPs tethered using the PMPDSAH brush had very little activity versus *S. aureus* or *P. aeruginosa*. Similar observations were made for Tet20-conjugated brushes, although the antimicrobial activity was considerably lower (Figure 3C,D).

Overall, the observations indicated a clear influence of the polymer brush chemistry and peptide structure on the antimicrobial activity of polymer-brush-tethered AMPs, with the tethered peptide activity decreasing in the order PDMA > PMPC > PMPDSAH.

3.3. Investigation of the Mechanism of Enhanced Antimicrobial Activity of Polymer-Brush-Tethered AMPs. Next we investigated potential mechanisms by which the polymer brush chemistry might affect the activity of tethered AMPs. AMPs are proposed to undergo changes to their secondary structure as they interact with bacterial membranes, resulting in membrane disruption and subsequent bacterial death.[51−54] To investigate whether changes in the secondary structure might account for differences in the activity of AMPs tethered using polymers with various chemical structures, we utilized CD spectroscopy. To study the interaction of polymer-

DOI: 10.1021/acsami.5b10074
ACS Appl. Mater. Interfaces 2015, 7, 28591−28605

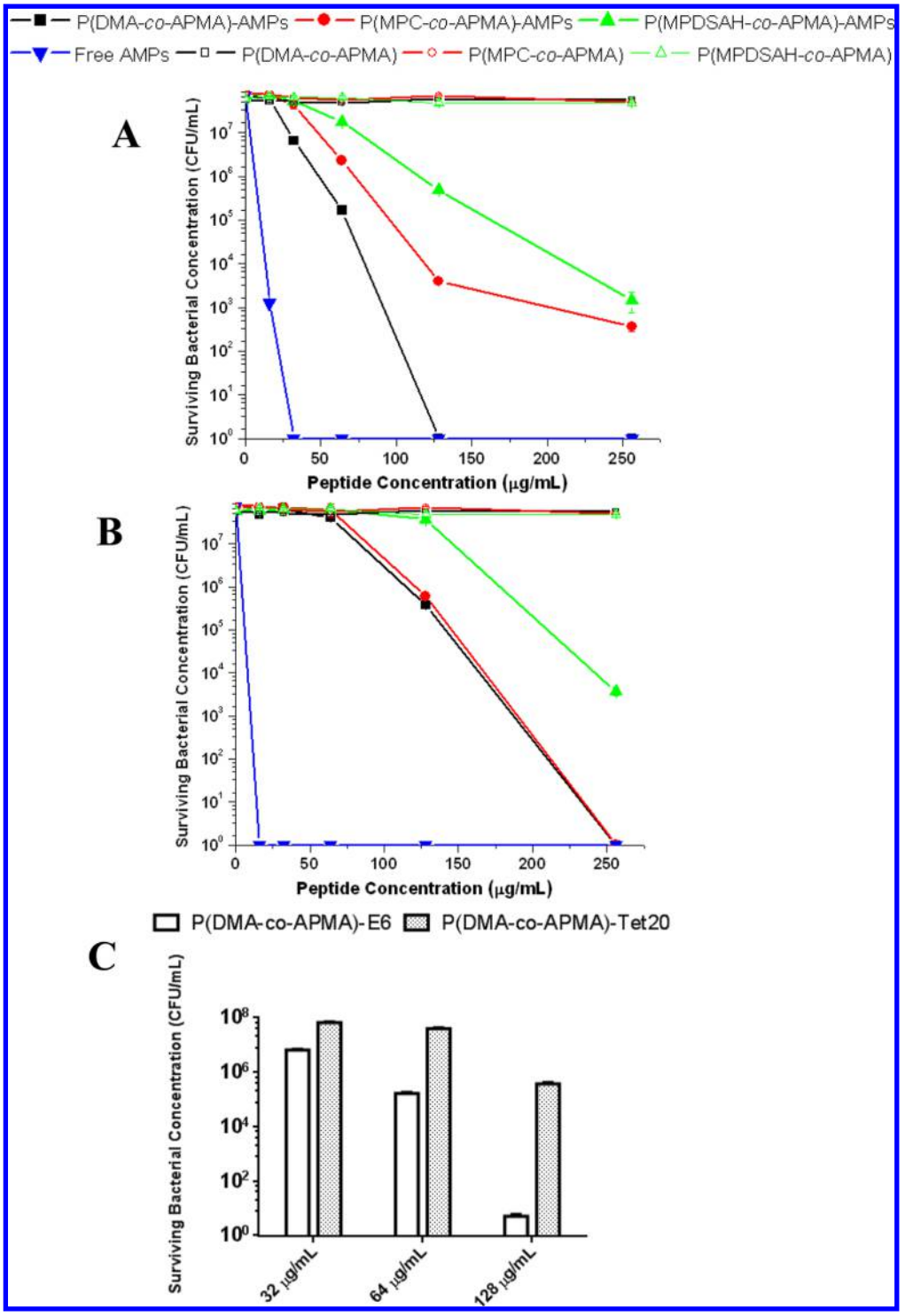

Figure 2. Comparison of the antimicrobial activity of tethered (A) E6 and (B) Tet20 to different brushes on NPs and soluble AMPs against *E. coli*. The control samples without AMPs were also shown. (C) Comparison of the antimicrobial activity of E6 with Tet20 tethered to PDMA-*co*-APMA brushes on NPs at different loading concentrations. The initial bacteria concentration was $3.6 \times 10^6 \pm 3 \times 10^5$ CFU/mL.

brush-tethered AMPs with a model bacterial biomembrane (DMPC/DMPG), we synthesized various polymer brushes on quartz slides and conjugated E6 to these brushes using chemistry similar to that described in section 3.1. The characteristics of E6-conjugated brushes on quartz slides are provided in Table 3. The grafting density of different brushes was controlled to a similar value, to allow a direct comparison of the peptide interaction with model biomembranes. Following peptide (E6) conjugation, brush thicknesses increased by 12, 6.4, and 8.1 nm, which corresponded to peptide densities of 1.08, 0.6, and 0.8 $\mu g/cm^2$ on PDMA-*co*-APMA, PMPC-*co*-APMA, and PMPDSAH-*co*-APMA brushes, respectively. The peptide conformation of E6 in both soluble as well as polymer-brush-tethered forms was determined using oriented CD spectroscopy in a buffer solution and in the presence of the model biomembrane. Figure 4A shows the CD spectra of soluble E6 before and after interaction with the lipid

DOI: 10.1021/acsami.5b10074
ACS Appl. Mater. Interfaces 2015, 7, 28591−28605

Table 2. MIC of Free (E6 and Tet20) and Tethered Peptides on the NP Surface

	MIC (μg/mL)		
	E. coli	*P. aeruginosa*	*S. aureus*
E6	32	16	32
Tet20	16	16	32
NPs−PDMA-*co*-APMA−E6	128	256	128
NPs−PDMA-*co*-APMA−Tet20	256	>256	>256
NPs−PMPC-*co*-APMA−E6	>256	256	256
NPs−PMPC-*co*-APMA−Tet20	256	>256	>256
NPs−PMPDSAH-*co*-APMA−E6	>256	>256	>256
NPs−PMPDSAH-*co*-APMA−Tet20	>256	>256	>256

membranes. Upon the addition of biomembranes, the peptide E6 changed its conformation with a prominent minimum at 220 nm, characteristic of β sheets. The secondary structure content of peptides in different environments was analyzed by fitting the spectra using two different programs (*CDSSTR* and *CONTINLL*). The data showed that biomembrane interaction caused the β sheet/turn structure of free E6 to increase by 38% while the unordered structure decreased by 37% (Table 5).

The characteristics of the raw spectra of E6, both in buffer solution and in the presence of a model biomembrane, changed with different polymers, indicating that different polymer brush chemistries contributed to the differences in the interaction of AMPs with a biomembrane (Figure 4B−D). Another important finding was that brush-tethered AMPs underwent lower degrees of conformational change compared with untethered AMP (Table 5). The β sheet/turn contents of tethered E6 on PDMA-*co*-APMA, PMPC-*co*-APMA, and PMPDSAH-*co*-APMA brushes increased by 6.2%, 4.1%, and 1.1%, respectively, with a corresponding decrease in the unordered structure. However, unlike soluble AMPs, polymer-brush-tethered peptides only underwent modest secondary structure changes upon interaction with biomembranes. The minor conformational change in the case of polymer-brush-tethered AMPs upon interaction with biomembranes may be due to the steric restriction associated with surface-grafted chains,[21,51] thus altering the way in which AMPs interact with the biomembrane. In addition, unlike soluble AMPs, polymer-brush-conjugated AMPs already had substantial secondary structure associated before their interaction with the model biomembrane (Table 5). This might also be contributing the minor conformational change upon interaction with lipid membranes.

3.4. Influence of the Polymer Brush Chemistry on the Viability of Surface-Adhered Bacteria. As is evident from the results in section 3.2, the efficiency of planktonic bacterial killing by polymer-brush-tethered AMPs on NPs was highly dependent on the brush chemistry. Both the antimicrobial activity of tethered peptides and the antiadhesion properties of the polymer brushes might contribute to the differences observed in the NP

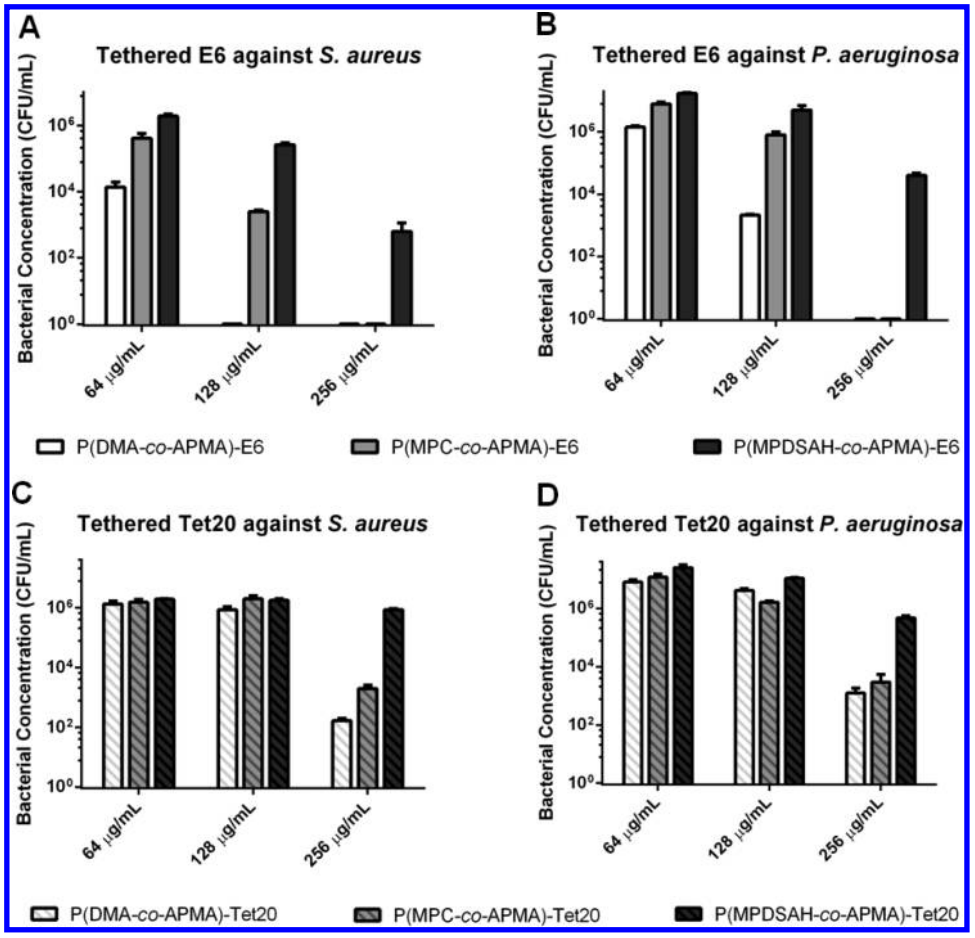

Figure 3. Influence of the polymer brush chemistry on the antimicrobial activity of tethered peptides. Antimicrobial activity of tethered E6 against (A) *S. aureus* and (B) *P. aeruginosa*. Antimicrobial activity of tethered Tet20 against (C) *S. aureus* and (D) *P. aeruginosa*. The initial bacteria concentrations of *S. aureus* and *P. aeruginosa* were $1.8 \times 10^6 \pm 1.5 \times 10^5$ and $3.8 \times 10^6 \pm 1.5 \times 10^5$ CFU/mL, respectively.

DOI: 10.1021/acsami.5b10074
ACS Appl. Mater. Interfaces 2015, 7, 28591−28605

Table 3. Characteristics of AMP E6-Tethered Polymer Brushes on Quartz Slides

sample	thickness (nm) before	thickness (nm) after	molecular weight, PDI	grafting density (chains/nm^2)	water contact angle after peptide E6 conjugation[a]
QS-*g*-PDMA-*co*-APMA	16.7 ± 0.9	27.8 ± 0.7	340000, 1.1	0.03	47.2 ± 4.6
QS-*g*-PMPC-*co*-APMA	19.1 ± 0.3	25.5 ± 0.5	350000, 1.3	0.033	52.1 ± 2.2
QS-*g*-PMPDSAH-*co*-APMA	17.5 ± 0.2	25.6 ± 0.3	380000,1.5	0.027	50.7 ± 5.3

[a]The initial water contact angles prior to peptide conjugation were as follows: QS−PDMA-*co*-APMA, 36.9 ± 0.9°; QS-PMPDSAH-*co*-APMA, 40.2 ± 1.9°; QS-PMPC-*co*-APMA, 40.7 ± 1.4°. PDI = polydispersity index.

Table 4. Characteristics of AMP E6-Tethered Polymer Brushes on Titanium Surfaces

sample	thickness (nm) before	thickness (nm) after	molecular weight, PDI	grafting density (chains/nm^2)	water contact angle after peptide E6 conjugation
Ti-*g*-PDMA-*co*-APMA	17.4 ± 0.7	28.3 ± 1.1	280000, 1.5	0.037	50.4 ± 2.7
Ti-*g*-PMPC-*co*-APMA	20.7 ± 2.0	27.1 ± 0.9	240000, 1.7	0.052	55.2 ± 0.7
Ti-*g*-PMPDSAH-*co*-APMA	17.3 ± 1.9	26.7 ± 1.5	220000, 1.5	0.047	52.6 ± 2.4

[a]The initial water contact angles prior to peptide conjugation were as follows: Ti−PDMA-*co*-APMA, 37.2 ± 2.2°; Ti−PMPC-*co*-APMA, 38.8 ± 2.5°; Ti−PMPDSAH-*co*-APMA, 37.9 ± 1.6°. PDI = polydispersity index.

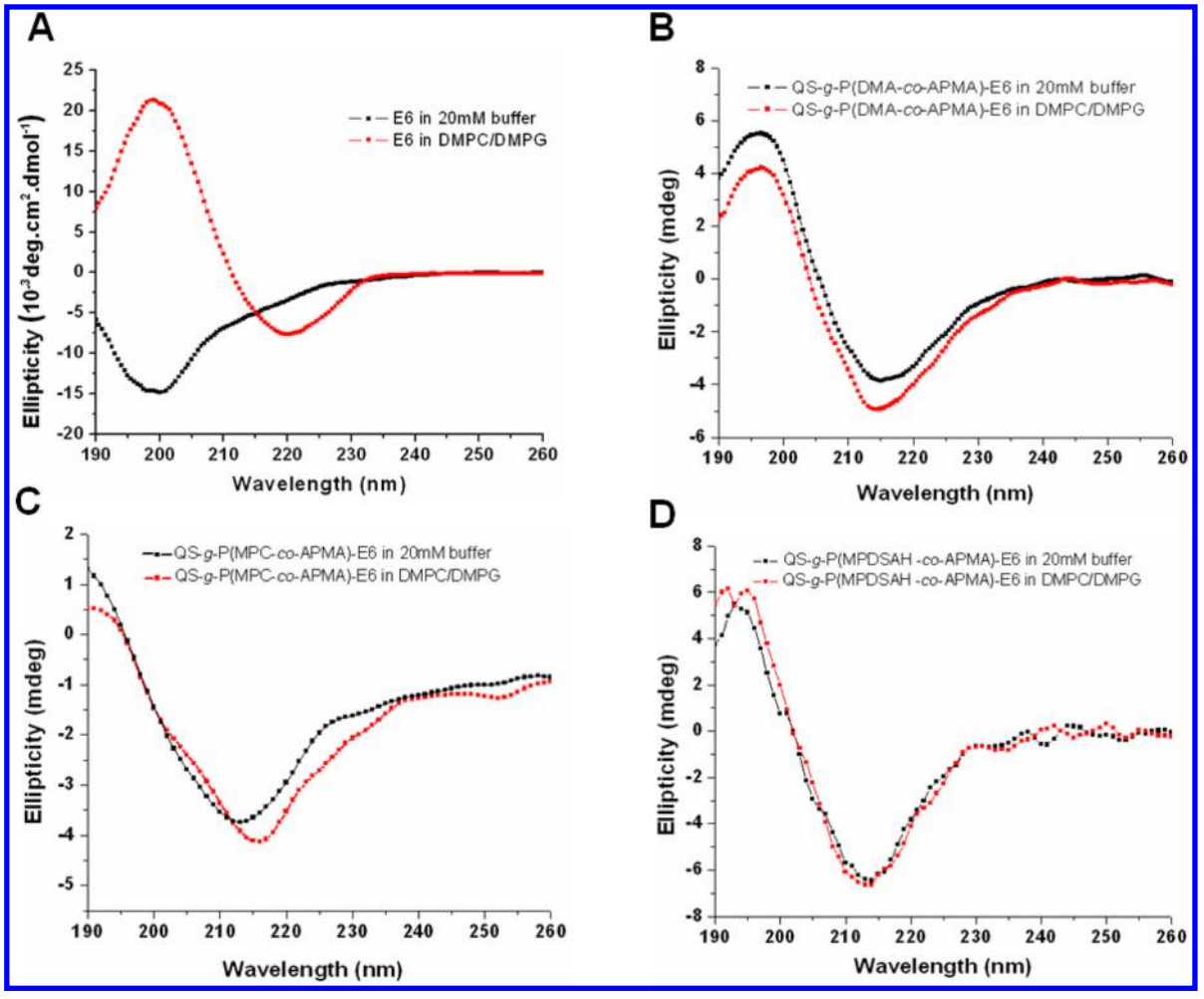

Figure 4. Biomembrane (1:1 DMPC/DMPG) interactions of (A) soluble E6 and of E6 tethered in (B) a PDMA-*co*-APMA brush, (C) a PMPC-*co*-APMA brush, and (D) a PMPDSAH-*co*-APMA brush.

model. To further validate the influence of the polymer brush chemistry on the antimicrobial activity of tethered peptides and to investigate the effects of the antiadhesion properties of the surface-grafted polymers, we used AMP-conjugated brushes on titanium surfaces. The characteristics of the coating and peptide density (E6) are given in Table 4. A Live/Dead BacLight bacterial assay was used to examine the degree of bacterial adhesion as well as the viability of adhered bacteria. In this assay, live bacteria appear green under fluorescence microscopy, while those with a disrupted membrane appear red. Figure 5 shows the

DOI: 10.1021/acsami.5b10074
ACS Appl. Mater. Interfaces 2015, 7, 28591−28605

Table 5. Changes in the Structural Content (%) of Peptide E6 and Polymer-Brush-Tethered E6 before and after Interaction with a Biomembrane (1:1 DMPC/DMPG)

		α helix	β sheet/ turn	unordered
E6	buffer	3.3 ± 0.3	40.5 ± 2.2	56 ± 3.7
	DMPC/ DMPG	1.8 ± 0.9	78.1 ± 4.6	19.5 ± 4
QS−PDMA-*co*-APMA-*g*-E6	buffer	6.3 ± 3.0	58.0 ± 7.1	35 ± 4.0
	DMPC/ DMPG	8.1 ± 2.8	64.2 ± 4.3	27.7 ± 3.9
QS−PMPC-*co*-APMA-*g*-E6	buffer	9.3 ± 3.0	53.3 ± 3.4	36.2 ± 5.9
	DMPC/ DMPG	8.0 ± 3.9	57.4 ± 5.0	34.7 ± 6.7
QS−PMPDSAH-*co*-APMA-*g*-E6	buffer	6.4 ± 1.0	57.5 ± 3.6	36.2 ± 4.5
	DMPC/ DMPG	5.9 ± 1.4	58.6 ± 4.9	35.1 ± 5.7

merged fluorescence images of live and dead cells on different polymer-brush-tethered E6 after incubation with *S. aureus*, and the respective images of live (green channel) and dead (red channel) cells are given in Figure S4 in the Supporting Information. As shown, the adherent bacteria on the PDMA brush conjugated with E6 appear more yellowish (due to a merge of red and green fluorescence) compared to those adhered to PMPC or PMPDSAH brushes. The percentages of dead bacteria (from the red channel) on brush-modified surfaces were calculated by dividing the number of bacteria stained in red by the total number of bacteria (from the merged image) on the surface. The percentages of dead bacteria on E6-tethered surfaces were 50.3%, 32.3%, and 22.5%, respectively, for PDMA, PMPC, and PMPDSAH brushes (Figure 6A). Increasing the initial bacteria concentration by 6-fold to a final bacteria concentration of about 10^8 CFU/mL did not show a major impact on the percentage of dead bacteria on the E6-conjugated brushes (Figure S5 in the Supporting Information). The percentage of dead bacteria on the bare titanium surface (control) was only around 13.3%, clearly demonstrating the killing efficiency of the AMP-conjugated PDMA brush system. Furthermore, these results clearly correlated with the killing efficiency observed for planktonic bacteria by AMP-conjugated NPs and relate to the biomembrane interaction described previously. Overall, the PDMA-brush-conjugated E6 was found to have the highest antibacterial efficiency.

The E6-modified PDMA brush was much more resistant to bacterial adhesion compared to the other AMP-modified brush systems (Figure 6B). In comparison to a bare titanium surface, a E6-conjugated PDMA brush on a titanium surface showed 46.9% reduction in bacterial adhesion, while E6-conjugated PMPC and PMPDSAH brushes showed only 7.6% and 13.2% reduction, respectively. Overall, these results clearly show the importance of selecting polymer brushes with the most favorable chemical characteristics to generate antimicrobial surfaces with the highest antimicrobial activity.

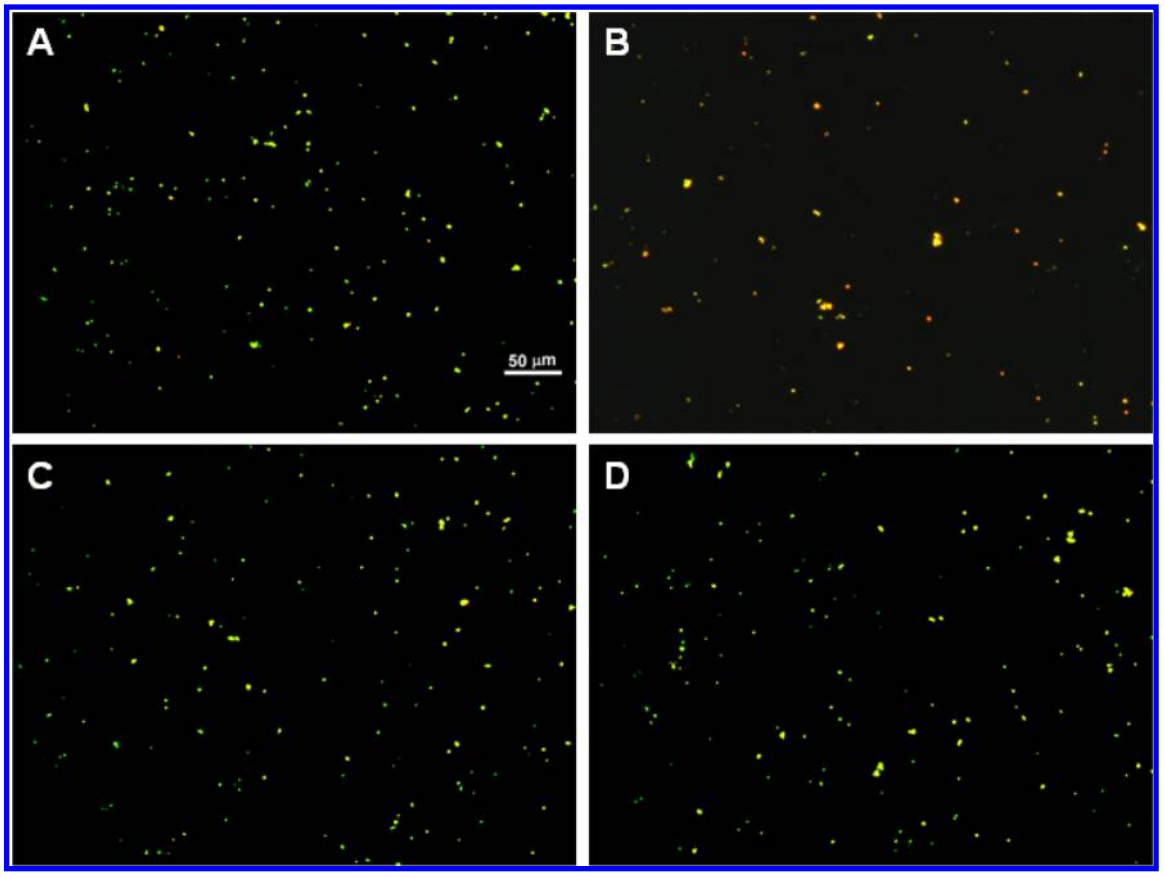

Figure 5. Representative fluorescence microscopy images of (A) bare titanium and (B) PDMA-*co*-APMA−E6-, (C) PMPC-*co*-APMA−E6-, and (D) PMPDSAH-*co*-APMA−E6-coated titanium surfaces by live/dead bacteria staining after a 4 h of incubation with *S. aureus*.

DOI: 10.1021/acsami.5b10074
ACS Appl. Mater. Interfaces 2015, 7, 28591−28605

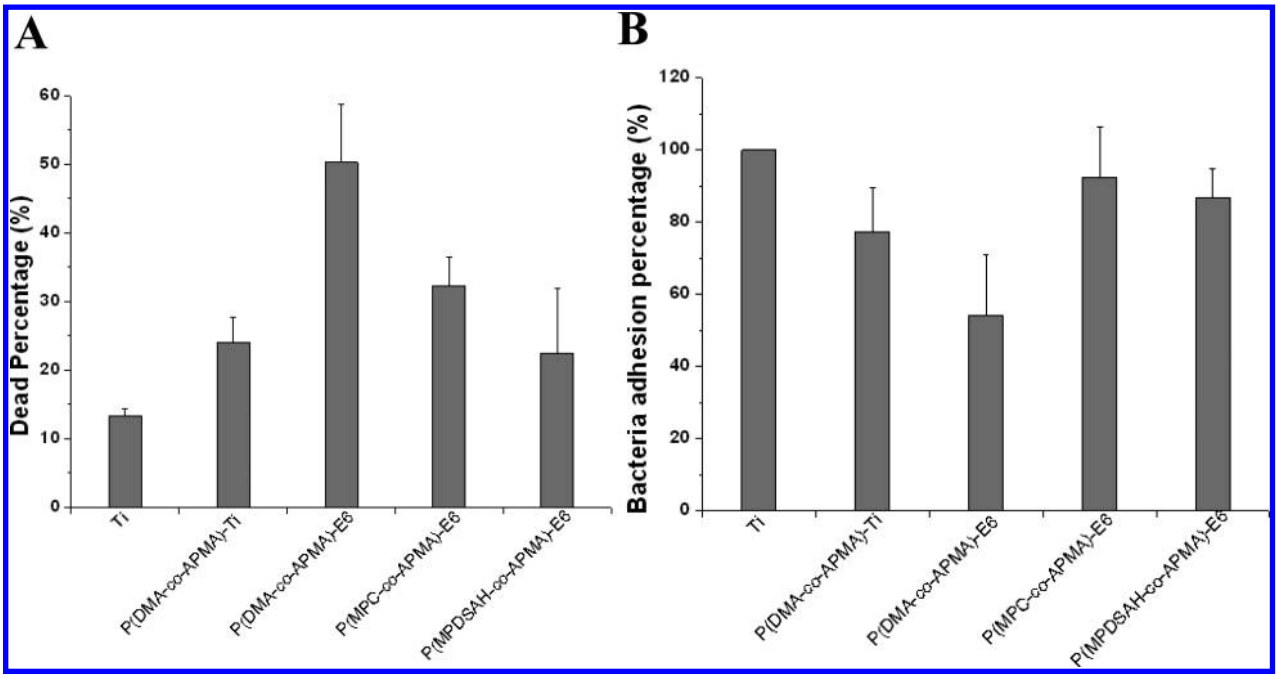

Figure 6. Antimicrobial activity (A) and reduction of bacterial (*S. aureus*) adhesion (B) on different brush surfaces tethered to E6. The percentage of dead bacteria was calculated as [number of dead bacteria (red channel)/total number of bacteria (counted from the merged image)] × 100. The percentage of adhered bacteria was calculated as (number of bacteria on a polymer brush or polymer brush peptide-tethered surface/number of bacteria on a bare titanium surface) × 100.

4. DISCUSSION

Tethering AMPs to polymer brushes has become an attractive approach for creating highly effective antimicrobial coatings because polymer brushes have high mechanical and chemical stability, excellent biocompatibility, and antifouling properties. The latter characteristic is very important because it prevents the accumulation of bacteria on the implant surface, thereby decreasing the formation of detrimental bacterial biofilms.[18−24] Furthermore, the flexibility of AMP-tethered polymer chains within the polymer brushes contributes significantly to retention of the antimicrobial activity of AMPs. While significant research has focused on a number of newly developed AMPs,[26−32] little consideration has been given to date to the potential impact of polymer brush chemistry and peptide structure on the bacterial adhesion and antimicrobial properties of the coatings. Given the fact that polymers and peptides are in very close proximity to each other within these novel coatings, we hypothesized that the chemical characteristics of both polymers and peptides would be important determinants to their overall antimicrobial and antifouling activities.

To address this issue, we synthesized AMP-tethered polymer brushes on different substrates using different combinations of polymers and AMPs. The grafting density of polymer brushes and peptides on each sample was controlled to be similar to allow for a direct comparison of various coatings. The AMP-conjugated brush coatings showed antimicrobial activity against both Gram-positive and Gram-negative bacteria, including *E. coli*, *S. aureus*, and *P. aeruginosa*. The AMPs conjugated to polymer brushes showed greater antimicrobial activity compared to surface-tethered systems that utilize other linkers or spacers. The greater antimicrobial activity observed for polymer-brush-tethered AMPs can be attributed to the higher lateral mobility and flexibility of tethered AMPs and increased coating density, thereby increasing the efficiency of the interaction with bacterial surfaces.[5,50] While this was known prior to the research undertaken here, our studies have now shown for the first time that, in addition to AMP characteristics, the polymer brush chemistry greatly influences the activity of tethered peptides. This finding illustrates the importance of the choice of linker for tethering peptides to surfaces because polymer brushes not only act as an attachment site but also directly aid bacterial killing. As shown here, there were considerable differences in the antimicrobial activity of the same tethered peptide on different brushes. Our studies have shown that conjugation of AMPs to PDMA brushes provided activity superior to that of the same AMPs attached to PMPC or PMPDSAH brushes. The observed antimicrobial activity was in the order PDMA > PMPC ≫ PMPDSAH. In addition, an AMP-tethered PDMA brush showed better efficiency against bacterial adherence, which is helpful in preventing the accumulation of bacterial debris on the surface, thereby not passivating the AMP action and providing a "regenerating" surface to kill bacteria.[8,21,22,55,56] The inverse correlation between the bacterial adhesion and killing efficiency (Figure 6) is not surprising because it has been postulated that surface-tethered AMPs can trigger an autolytic and/or cell death mechanism by generating a disturbance of surface electrostatics at the bacterial surface.[38,54,57] A short surface contact time between tethered AMP and bacteria might be sufficient to kill the bacteria. Thus, a coating that uses multiple mechanisms to prevent bacterial deposition on surfaces and/or to rapidly kill is beneficial because it would significantly decrease the amount of deposited bacteria or bacterial debris that might interfere with the activity of AMPs by shielding their interaction with the bacteria.

AMP-mediated killing likely requires the direct interaction of peptide with the bacterial surface, as described previously. The charge of the peptide is a very important determinant in the initial interaction, with negatively charged bacteria being more attracted to positively charged AMPs, resulting in membrane disruption. Considering the fact that all of the peptides studied

DOI: 10.1021/acsami.5b10074
ACS Appl. Mater. Interfaces 2015, 7, 28591−28605

here were polycationic in nature, the differences in the attraction of tethered peptides for the bacterial membranes cannot account for the differences in the antimicrobial activities observed for different polymer systems studied here. Instead, it may be the relative positioning of charged and hydrophobic residues[38] that impact events subsequent to the initial surface binding that contributes to such differences. The CD measurements performed provided some insight into these events, suggesting that the differences in the antimicrobial activity might relate to the extent of change in the secondary structure of the conjugated AMPs. Tethered peptides assumed a much more ordered peptide structure upon interaction with biomembranes compared to their soluble counterparts. Further support for this concept came from the finding that E6 tethered to PDMA (the most potent antimicrobial and antifouling combination), underwent the greatest change in the secondary structure upon interaction with synthetic biomembranes. Because the antibacterial effect of this class of immobilized peptides does not depend on the membrane penetration ability,[38,43] small changes in the peptide secondary structure might be sufficient to provide antimicrobial activity, as demonstrated in the case of the PDMA−E6 brush system. Conversely, E6 tethered to the PMPDSAH brush did not undergo any noticeable change in the secondary structure at similar peptide loading density and was the least active peptide-conjugated brush system. We suggest therefore that the lack of change in the secondary structure for E6 when tethered to the PMPDSAH brush might result from electrostatic interactions between the zwitterionic PMPDSAH and the positively charged peptide E6, interfering with the interaction of the peptide with the biomembrane. Isothermal titration calorimetry (ITC) experiments, however, did not support this hypothesis, in that they showed that there was no interaction between PMPDSAH and E6 (Figure S6 in the Supporting Information). The small differences in the peptide loading density may have an influence on the changes in the secondary structure of tethered E6 on polymer brushes; however, this needs further exploration. Nevertheless, the presentation of AMP at close proximity, such as in the case of a polymer brush, might offer a different environment, and we cannot completely rule out such arguments.

Furthermore, the differences in the antimicrobial activity and bacterial adhesion are unlikely to be due to the surface hydrophilicity differences because the water contact angles on these surfaces were very similar (Table 2). The surface roughness of E6 and Tet20 surfaces was less than 2 nm, which does not influence the water contact angle of AMP-tethered polymer brushes (Figure S7 in the Supporting Information). Another plausible reason might be due to the differential distribution of AMPs within the surface-grafted brushes. Given the way that the polymer brush system is structured, the restricted diffusion of large molecules within the brush layer might yield a higher peptide density near the outer surface of the brushes.[51] This higher local concentration of peptides might have translated into a higher relative number of peptides being exposed to the bacterial surface, thereby resulting in greater secondary structure changes. Conversely, tethered peptides buried deep within the brush layer would not be sterically capable of interacting with bacteria or the artificial biomembrane, especially because the peptides used in this study were quite small. Regardless of this, we have identified a highly effective candidate to move forward, the E6-tethered PDMA brush, which provides highly effective antibacterial and antifouling activities.

Another important parameter that must be considered when choosing candidate AMPs for the development of novel coatings is the peptide structure, which considerably affects the activity of soluble peptides and from the studies presented here seems to be influential in the activity of tethered peptides. Figures 2 and 3 show that different AMPs behaved very differently when conjugated to the same polymer brush. This was illustrated by the fact that tethered E6 was much more effective than tethered Tet20, even though the soluble Tet20 showed more potent bactericidal activity than E6. This could be due to the difference in the killing mechanism between soluble and immobilized AMPs.[28−36,38] For the soluble AMPs, it was proposed that the AMPs interact with negatively charged lipid head groups of the outer bacterial surfaces, which leads to membrane perturbation and disruption or translocation across the cytoplasmic membrane to attack cytoplasmic targets.[28−36] For tethered AMPs, the high positive charge density on the surface leads to depolarization of the membrane, which may introduce an electrostatic imbalance across the membrane and trigger a lethal event such as activation of the autolytic enzymes or disruption of the ionic balance of more-internal layers.[38] The difference in the killing mechanism between soluble and tethered antimicrobial agents other than AMPs has also been observed recently.[58,59] The peptide sequence, peptide density, surface hydrophobicity, and positioning of the residues relative to the tethering point likely all contribute to the differences in the antimicrobial activity observed.[21,22,37,54] Compared to Tet20, E6 has more hydrophobic residues located in the middle, away from the conjugation site, which is favorable to form direct contact with bacteria.[38] Critically, the peptide density (or positive charge density) of tethered E6 was 1.5-fold higher than that of tethered Tet20 for all of the systems studied (Table 1), and the efficiency of tethering might indeed reflect, in part, the physical properties of the peptide and account for the increased antibacterial activity. Higher peptide (or positive charge) density has previously been shown to be favorable for inhibiting bacterial growth and making it a better antibacterial surface.[23,37,58,59]

Another important factor in the design of effective polymer-brush-based coatings is the swelling of the AMP-tethered brush because greater swelling might result in the exposure of more peptides to the surrounding environment, thereby increasing the chance for effective peptide/bacterial membrane interactions. A comparison of the swelling ratio of AMP-conjugated brushes (ratio of wet thickness in aqueous conditions to dry thickness) showed a slight decrease (Table S1 in the Supporting Information) after conjugation of AMPs. We do not believe that this explains the differences in activity observed between E6- and Tet20-containing brushes because the actual decrease in swelling was very similar after conjugation of both peptides, but E6 had greater antibacterial activity. A similar swelling ratio of AMP-tethered brushes also indicated that both E6- and Tet20-modified surfaces had similar freedom to interact with the bacterial surface. In addition, the tethered E6 surface was more hydrophilic (water contact angle: 46.3 ± 4.2°) than the Tet20 surface (water contact angle: 66.3 ± 2.3°), which might influence the retention of dead bacteria on the surface, making the tethered peptide E6 more accessible to viable bacteria. Our recent study also showed that surfaces possessing a relatively higher hydrophilic character exhibited better antimicrobial properties and inhibited biofilm formation the most.[21,22]

While we have confirmed previous findings that linker flexibility is an important determinant of tethered AMP activity,[19,47,50] our study expands on this to show that the

DOI: 10.1021/acsami.5b10074
ACS Appl. Mater. Interfaces 2015, 7, 28591−28605

specific chemistry of both the linker and peptide is the most important factor to be considered in the development of novel antimicrobial surface coatings. In addition, the hydrophilicity of AMP-conjugated brushes is also important because it might strongly influence the antiadhesion properties of the coatings while enhancing the antimicrobial activity. Therefore, a fine balance between the two needs to be accomplished.

5. CONCLUSIONS

We synthesized AMP-tethered polymer brushes using the combination of three different nonfouling polymers and two AMPs with high antimicrobial activity on different substrates ranging from NPs to flat surfaces. Tethered peptides were found to exert different antimicrobial activities compared to their soluble counterparts. Overall, we found that the brush structure is one determinant for effective AMP activity on surfaces. Specifically, we found that the polymer chemistry greatly influences the plasticity of the secondary structure of the tethered peptides, with significant consequences to the overall antibacterial activity. The peptide density and surface hydrophilicity were also suggested to contribute to the differences in the antimicrobial activities of the surfaces. While the findings of the current paper focused mainly on the interplay between polymers and AMPs, it is highly likely that similar interactions also take place between AMPs and other types of coatings. As such, the design of novel coatings utilizing tethered AMP technology should carefully consider the polymer chemistry and AMP characteristics to provide the most potent antimicrobial and antifouling surface coating.

■ ASSOCIATED CONTENT

Supporting Information

The Supporting Information is available free of charge on the ACS Publications website at DOI: 10.1021/acsami.5b10074.

Data on the synthesis of PDMA-*co*-APMA brushes on a titanium surface, NMR spectra of copolymers in solution and on the surface, inhibition of luminescence of *E. coli* upon incubation with NPs modified with peptides, fluorescence and confocal microscopy images of bacterial adhesion on a titanium surface grafted with peptides, ITC binding measurement between PMPDSAH and E6, the surface morphology of a titanium surface grafted with peptides, an XPS survey scan, and characterization of AMP tethered polymer brushes on a silicon substrate (PDF)

■ AUTHOR INFORMATION

Corresponding Author

*Phone: 604 822 7085. E-mail: jay@pathology.ubc.ca.

Notes

The authors declare no competing financial interest.

■ ACKNOWLEDGMENTS

This research was funded by the Canadian Institutes of Health Research (CIHR) and Natural Science and Engineering Research Council of Canada. The authors thank the LMB Macromolecular Hub at the University of British Columbia Centre for Blood Research for use of the analytical facilities. The infrastructure facility is supported by the Canada Foundation for Innovation and the Michael Smith Foundation of Health Research (MSFHR). E.F.H. was supported by a postdoctoral fellowship from the CIHR. J.N.K. is the recipient of a Career Investigator Scholar award from MSFHR. R.E.W.H. holds a Canada Research Chair in new anti-infective drug discovery.

■ REFERENCES

(1) Hetrick, E. M.; Schoenfisch, M. H. Reducing Implant-Related Infections: Active Release Strategies. *Chem. Soc. Rev.* **2006**, *35*, 780−789.
(2) Darouiche, R. O. Current Concepts - Treatment of Infections Associated with Surgical Implants. *N. Engl. J. Med.* **2004**, *350*, 1422−1429.
(3) Klevens, R. M.; Edwards, J. R.; Richards, C. L.; Horan, T. C.; Gaynes, R. P.; Pollock, D. A.; Cardo, D. M. Estimating Health Care-Associated Infections and Deaths in US Hospitals, 2002. *Public Health Rep.* **2007**, *122*, 160−166.
(4) Grainger, D. W.; van der Mei, H. C.; Jutte, P. C.; van den Dungen, J.; Schultz, M. J.; van der Laan, B.; Zaat, S. A. J.; Busscher, H. J. Critical Factors in the Translation of Improved Antimicrobial Strategies for Medical Implants and Devices. *Biomaterials* **2013**, *34*, 9237−9243.
(5) Onaizi, S. A.; Leong, S. S. J. Tethering antimicrobial peptides: Current Status and Potential Challenges. *Biotechnol. Adv.* **2011**, *29*, 67−74.
(6) Costa, F.; Carvalho, I. F.; Montelaro, R. C.; Gomes, P.; Martins, M. C. L. Covalent Immobilization of Antimicrobial Peptides (AMPs) onto Biomaterial Surfaces. *Acta Biomater.* **2011**, *7*, 1431−1440.
(7) Lo, J.; Lange, D.; Chew, B. Ureteral Stents and Foley Catheters-Associated Urinary Tract Infections: the Role of Coatings and Materials in Infection Prevention. *Antibiotics* **2014**, *3*, 87−97.
(8) Hadjesfandiari, N.; Yu, K.; Mei, Y.; Kizhakkedathu, J. N. Polymer Brush-Based Approaches for the Development of Infection-Resistant Surfaces. *J. Mater. Chem. B* **2014**, *2*, 4968−4978.
(9) Nejadnik, M. R.; van der Mei, H. C.; Norde, W.; Busscher, H. J. Bacterial Adhesion and Growth on a Polymer Brush-Coating. *Biomaterials* **2008**, *29*, 4117−4121.
(10) Cho, W. K.; Kong, B. Y.; Choi, I. S. Highly Efficient Non-Biofouling Coating of Zwitterionic Polymers: Poly((3-(methacryloylamino)propyl)-dimethyl(3-sulfopropyl)ammonium hydroxide). *Langmuir* **2007**, *23*, 5678−5682.
(11) Cheng, G.; Zhang, Z.; Chen, S. F.; Bryers, J. D.; Jiang, S. Y. Inhibition of Bacterial Adhesion and Biofilm Formation on Zwitterionic Surfaces. *Biomaterials* **2007**, *28*, 4192−4199.
(12) Smith, R. S.; Zhang, Z.; Bouchard, M.; Li, J.; Lapp, H. S.; Brotske, G. R.; Lucchino, D. L.; Weaver, D.; Roth, L. A.; Coury, A.; Biggerstaff, J.; Sukavaneshvar, S.; Langer, R.; Loose, C. Vascular Catheters with a Nonleaching Poly-Sulfobetaine Surface Modification Reduce Thrombus Formation and Microbial Attachment. *Sci. Transl. Med.* **2012**, *4*, 153ra132.
(13) Hirota, K.; Murakami, K.; Nemoto, K.; Miyake, Y. Coating of a Surface with 2-Methacryloyloxyethyl Phosphorylcholine (MPC) Co-Polymer Significantly Reduces Retention of Human Pathogenic Microorganisms. *FEMS Microbiol. Lett.* **2005**, *248*, 37−45.
(14) Yang, W. J.; Cai, T.; Neoh, K. G.; Kang, E. T.; Teo, S. L. M.; Rittschof, D. Barnacle Cement as Surface Anchor for "Clicking" of Antifouling and Antimicrobial Polymer Brushes on Stainless Steel. *Biomacromolecules* **2013**, *14*, 2041−2051.
(15) Hu, R.; Li, G. Z.; Jiang, Y. J.; Zhang, Y.; Zou, J. J.; Wang, L.; Zhang, X. W. Silver-Zwitterion Organic-Inorganic Nanocomposite with Antimicrobial and Antiadhesive Capabilities. *Langmuir* **2013**, *29*, 3773−3779.
(16) Wu, H. X.; Tan, L.; Tang, Z. W.; Yang, M. Y.; Xiao, J. Y.; Liu, C. J.; Zhuo, R. X. Highly Efficient Antibacterial Surface Grafted with a Triclosan-Decorated Poly(N-Hydroxyethylacrylamide) Brush. *ACS Appl. Mater. Interfaces* **2015**, *7*, 7008−7015.
(17) Muszanska, A. K.; Busscher, H. J.; Herrmann, A.; van der Mei, H. C.; Norde, W. Pluronic-Lysozyme Conjugates as Anti-Adhesive and Antibacterial Bifunctional Polymers for Surface Coating. *Biomaterials* **2011**, *32*, 6333−6341.
(18) Yang, W. J.; Cai, T.; Neoh, K. G.; Kang, E. T.; Dickinson, G. H.; Teo, S. L. M.; Rittschof, D. Biomimetic Anchors for Antifouling and Antibacterial Polymer Brushes on Stainless Steel. *Langmuir* **2011**, *27*, 7065−7076.

DOI: 10.1021/acsami.5b10074
ACS Appl. Mater. Interfaces 2015, 7, 28591−28605

(19) Glinel, K.; Jonas, A. M.; Jouenne, T.; Leprince, J.; Galas, L.; Huck, W. T. S. Antibacterial and Antifouling Polymer Brushes Incorporating Antimicrobial Peptide. *Bioconjugate Chem.* **2009**, *20*, 71−77.
(20) Laloyaux, X.; Fautre, E.; Blin, T.; Purohit, V.; Leprince, J.; Jouenne, T.; Jonas, A. M.; Glinel, K. Temperature-Responsive Polymer Brushes Switching from Bactericidal to Cell-repellent. *Adv. Mater.* **2010**, *22*, 5024−5028.
(21) Gao, G. Z.; Lange, D.; Hilpert, K.; Kindrachuk, J.; Zou, Y. Q.; Cheng, J. T. J.; Kazemzadeh-Narbat, M.; Yu, K.; Wang, R. Z.; Straus, S. K.; Brooks, D. E.; Chew, B. H.; Hancock, R. E. W.; Kizhakkedathu, J. N. The Biocompatibility and Biofilm Resistance of Implant Coatings Based on Hydrophilic Polymer Brushes Conjugated with Antimicrobial Peptides. *Biomaterials* **2011**, *32*, 3899−3909.
(22) Gao, G. Z.; Yu, K.; Kindrachuk, J.; Brooks, D. E.; Hancock, R. E. W.; Kizhakkedathu, J. N. Antibacterial Surfaces Based on Polymer Brushes: Investigation on the Influence of Brush Properties on Antimicrobial Peptide Immobilization and Antimicrobial Activity. *Biomacromolecules* **2011**, *12*, 3715−3727.
(23) Godoy-Gallardo, M.; Mas-Moruno, C.; Yu, K.; Manero, J. M.; Gil, F. J.; Kizhakkedathu, J. N.; Rodriguez, D. Antibacterial Properties of hLf1−11 Peptide onto Titanium Surfaces: a Comparison Study between Silanization and Surface Initiated Polymerization. *Biomacromolecules* **2015**, *16*, 483−496.
(24) Li, X.; Li, P.; Saravanan, R.; Basu, A.; Mishra, B.; Lim, S. H.; Su, X. D.; Tambyah, P. A.; Leong, S. S. J. Antimicrobial Functionalization of Silicone Surfaces with Engineered Short Peptides Having Broad Spectrum Antimicrobial and Salt-Resistant Properties. *Acta Biomater.* **2014**, *10*, 258−266.
(25) Basu, A.; Mishra, B.; Leong, S. S. J. Immobilization of Polybia-MPI by Allyl Glycidyl Ether Based Brush Chemistry to Generate a Novel Antimicrobial Surface. *J. Mater. Chem. B* **2013**, *1*, 4746−4755.
(26) Mishra, B.; Basu, A.; Chua, R. R. Y.; Saravanan, R.; Tambyah, P. A.; Ho, B.; Chang, M. W.; Leong, S. S. J. Site Specific Immobilization of a Potent Antimicrobial Peptide onto Silicone Catheters: Evaluation against Urinary Tract Infection Pathogens. *J. Mater. Chem. B* **2014**, *2*, 1706−1716.
(27) Lo, J. C. Y.; Lange, D. Current and Potential Applications of Host-Defense Peptides and Proteins in Urology. *BioMed Res. Int.* **2015**, *2015*, 189016.
(28) Hancock, R. E. W.; Sahl, H. G. Antimicrobial and Host-Defense Peptides as New Anti-infective Therapeutic Strategies. *Nat. Biotechnol.* **2006**, *24*, 1551−1557.
(29) Fjell, C. D.; Hiss, J. A.; Hancock, R. E. W.; Schneider, G. Designing Antimicrobial Peptides: Form Follows Function. *Nat. Rev. Drug Discovery* **2011**, *11*, 37−51.
(30) Jenssen, H.; Hamill, P.; Hancock, R. E. W. Peptide Antimicrobial Agents. *Clin. Microbiol. Rev.* **2006**, *19*, 491−511.
(31) Zasloff, M. Antimicrobial Peptides of Multicellular Organisms. *Nature* **2002**, *415*, 389−395.
(32) Brogden, K. A. Antimicrobial Peptides: Pore Formers or Metabolic Inhibitors in Bacteria? *Nat. Rev. Microbiol.* **2005**, *3*, 238−250.
(33) Boman, H. G. Antibacterial Peptides: Basic Facts and Emerging Concepts. *J. Intern. Med.* **2003**, *254*, 197−215.
(34) Bechinger, B.; Salnikov, E. S. The Membrane Interactions of Antimicrobial Peptides Revealed by Solid-state NMR Spectroscopy. *Chem. Phys. Lipids* **2012**, *165*, 282−301.
(35) Melo, M. N.; Ferre, R.; Castanho, M. Opinion: Antimicrobial Peptides: Linking Partition, Activity and High Membrane-bound Concentrations. *Nat. Rev. Microbiol.* **2009**, *7*, 245−250.
(36) Nguyen, L. T.; Haney, E. F.; Vogel, H. J. The Expanding Scope of Antimicrobial Peptide Structures and Their Modes of Action. *Trends Biotechnol.* **2011**, *29*, 464−472.
(37) Costa, F.; Maia, S. R.; Gomes, P.A. C.; Martins, M. C. L. Dhvar5 Antimicrobial Peptide (AMP) Chemoselective Covalent Immobilization Results on Higher Antiadherence Effect than Simple Physical Adsorption. *Biomaterials* **2015**, *52*, 531−538.
(38) Hilpert, K.; Elliott, M.; Jenssen, H.; Kindrachuk, J.; Fjell, C. D.; Korner, J.; Winkler, D. F. H.; Weaver, L. L.; Henklein, P.; Ulrich, A. S.; Chiang, S. H. Y.; Farmer, S. W.; Pante, N.; Volkmer, R.; Hancock, R. E. W. Screening and Characterization of Surface-Tethered Cationic Peptides for Antimicrobial Activity. *Chem. Biol.* **2009**, *16*, 58−69.
(39) Matyjaszewski, K.; Miller, P. J.; Shukla, N.; Immaraporn, B.; Gelman, A.; Luokala, B. B.; Siclovan, T. M.; Kickelbick, G.; Vallant, T.; Hoffmann, H.; Pakula, T. Polymers at Interfaces: Using Atom Transfer Radical Polymerization in the Controlled Growth of Homopolymers and Block Copolymers from Silicon Surfaces in the Absence of Untethered Sacrificial Initiator. *Macromolecules* **1999**, *32*, 8716−8724.
(40) Kizhakkedathu, J. N.; Brooks, D. E. Synthesis of Poly(N,N-dimethylacrylamide) Brushes from Charged Polymeric Surfaces by Aqueous ATRP: Effect of Surface Initiator Concentration. *Macromolecules* **2003**, *36*, 591−598.
(41) Berti, L.; D'Agostino, P. S.; Boeneman, K.; Medintz, I. L. Improved Peptidyl Linkers for Self-assembly of Semiconductor Quantum Dot Bioconjugates. *Nano Res.* **2009**, *2*, 121−129.
(42) Barbey, R.; Lavanant, L.; Paripovic, D.; Schuwer, N.; Sugnaux, C.; Tugulu, S.; Klok, H. A. Polymer Brushes via Surface-initiated Controlled Radical Polymerization: Synthesis, Characterization, Properties and Applications. *Chem. Rev.* **2009**, *109*, 5437−5527.
(43) Hilpert, K.; Volkmer-Engert, R.; Walter, T.; Hancock, R. E. W. High-Throughput Generation of Small Antibacterial Peptides with Improved Activity. *Nat. Biotechnol.* **2005**, *23*, 1008−1012.
(44) Netuschil, L.; Auschill, T. M.; Sculean, A.; Arweiler, N. B. Confusion over Live/Dead Stainings for the Detection of Vital Microorganisms in Oral Biofilms - Which Stain is Suitable? *BMC Oral Health* **2014**, *14*, 2.
(45) Stiefel, P.; Schmidt-Emrich, S.; Maniura-Weber, K.; Ren, Q. Critical Aspects of Using Bacterial Cell Viability Assays with the Fluorophores SYTO9 and Propidium iodide. *BMC Microbiol.* **2015**, *15*, 36.
(46) Yu, K.; Lai, B. F. L.; Gani, J.; Mikut, R.; Hilpert, K.; Kizhakkedathu, J. N. Interaction of Blood Components with Cathelicidins and Their Modified Versions. *Biomaterials* **2015**, *69*, 201−211.
(47) Bagheri, M.; Beyermann, M.; Dathe, M. Immobilization Reduces the Activity of Surface-Bound Cationic Antimicrobial Peptides with No Influence upon the Activity Spectrum. *Antimicrob. Agents Chemother.* **2009**, *53*, 1132−1141.
(48) Haynie, S. L.; Crum, G. A.; Doele, B. A. Antimicrobial Activities of Amphiphilic Peptides Covalently Bonded to a Water-Insoluble Resin. *Antimicrob. Agents Chemother.* **1995**, *39*, 301−307.
(49) Cho, W. M.; Joshi, B. P.; Cho, H.; Lee, K. H. Design and Synthesis of Novel Antibacterial Peptide-Resin Conjugates. *Bioorg. Med. Chem. Lett.* **2007**, *17*, 5772−5776.
(50) Gabriel, M.; Nazmi, K.; Veerman, E. C.; Amerongen, A. V. N.; Zentner, A. Preparation of LL-37-Grafted Titanium Surfaces with Bactericidal Activity. *Bioconjugate Chem.* **2006**, *17*, 548−550.
(51) Gao, G.; Cheng, J. T. J.; Kindrachuk, J.; Hancock, R. E. W.; Straus, S. K.; Kizhakkedathu, J. N. Biomembrane Interactions Reveal the Mechanism of Action of Surface-immobilized Host Defense IDR-1010 Peptide. *Chem. Biol.* **2012**, *19*, 199−209.
(52) Wieczorek, M.; Jenssen, H.; Kindrachuk, J.; Scott, W. R. P.; Elliott, M.; Hilpert, K.; Cheng, J. T. J.; Hancock, R. E. W.; Straus, S. K. Structural Studies of a Peptide with Immune Modulating and Direct Antimicrobial Activity. *Chem. Biol.* **2010**, *17*, 970−980.
(53) Kumar, P.; Shenoi, R. A.; Lai, B. F. L.; Nguyen, M.; Kizhakkedathu, J. N.; Straus, S. K. Conjugation of Aurein 2.2 to HPG Yields an Antimicrobial with Better Properties. *Biomacromolecules* **2015**, *16*, 913−923.
(54) Resende, J. M.; Moraes, C. M.; Munhoz, V. H. O.; Aisenbrey, C.; Verly, R. M.; Bertani, P.; Cesar, A.; Pilo-Veloso, D.; Bechinger, B. Membrane Structure and Conformational Changes of the Antibiotic Heterodimeric Peptide Distinctin by Solid-state NMR Spectroscopy. *Proc. Natl. Acad. Sci. U. S. A.* **2009**, *106*, 16639−16644.
(55) Mi, L.; Jiang, S. Y. Integrated Antimicrobial and Nonfouling Zwitterionic Polymers. *Angew. Chem., Int. Ed.* **2014**, *53*, 1746−1754.
(56) Yao, F.; Fu, G. D.; Zhao, J. P.; Kang, E. T.; Neoh, K. G. Antibacterial Effect of Surface-functionalized Polypropylene Hollow

DOI: 10.1021/acsami.5b10074
ACS Appl. Mater. Interfaces 2015, 7, 28591−28605

Fiber Membrane from Surface-initiated Atom Transfer Radical Polymerization. *J. Membr. Sci.* **2008**, *319*, 149−157.
(57) Jelokhani-Niaraki, M.; Prenner, E. J.; Kay, C. M.; McElhaney, R. N.; Hodges, R. S. Conformation and Interaction of the Cyclic Cationic Antimicrobial Peptides in Lipid Bilayers. *J. Pept. Res.* **2002**, *60*, 23−36.
(58) Asri, L.; Crismaru, M.; Roest, S.; Chen, Y.; Ivashenko, O.; Rudolf, P.; Tiller, J. C.; van der Mei, H. C.; Loontjens, T. J. A.; Busscher, H. J. A Shape- Adaptive, Antibacterial- Coating of Immobilized Quaternary-Ammonium Compounds Tethered on Hyperbranched Polyurea and its Mechanism of Action. *Adv. Funct. Mater.* **2014**, *24*, 346−355.
(59) Roest, S.; van der Mei, H. C.; Loontjens, T. J. A.; Busscher, H. J. Charge Properties and Bacterial Contact-Killing of Hyperbranched Polyurea-Polyethyleneimine Coatings with Various Degrees of Alkylation. *Appl. Surf. Sci.* **2015**, *356*, 325−332.
(60) Yu, K.; Lai, B. F. L.; Foley, J. H.; Krisinger, M. J.; Conway, E. M.; Kizhakkedathu, J. N. Modulation of Complement Activation and Amplification on Nanoparticle Surfaces by Glycopolymer Conformation and Chemistry. *ACS Nano* **2014**, *8*, 7687−7703.

DOI: 10.1021/acsami.5b10074
ACS Appl. Mater. Interfaces 2015, 7, 28591−28605